High-Resolution Infrared Study of Hydrogen (1×1) on Tungsten (100)

Y. J. Chabal[(a)] and A. J. Sievers
Laboratory of Atomic and Solid State Physics and Materials Science Center, Cornell University, Ithaca, New York 14853
(Received 17 December 1979)

The first high-resolution observation of the ν_1 vibrational mode of H chemisorbed on W(100) at saturation coverage has been obtained by surface electromagnetic wave spectroscopy.

PACS numbers: 68.30.+z, 78.30.Er

Vibrational modes of H on W(100) have recently been detected by high-resolution electron energy-loss spectroscopy (ELS).[1-4] In both the low-coverage β_2 phase and the high-coverage β_1 phase hydrogen atoms are situated on bridge positions.[3] At low coverage, $\theta \leq 0.5$, the W atoms are reconstructed along the (11) direction and the H atoms are located above the two closest W atoms. The normal mode perpendicular to the surface has a vibrational frequency centered near 155 meV (1250 cm^{-1}). As the coverage increases towards saturation, $\theta = 2$, the hydrogen induces the surface W atoms back into registry with the bulk lattice, the bridge angle increases, and the center frequency of the normal mode decreases to about 130 meV (1050 cm^{-1}). Two high-resolution ELS experiments[1,2] have resolved the vibrational line widths at both coverages. More precisely, Adnot and Carette[2] find a vibrational width of 7.5 meV (60 cm^{-1}) for the 155-meV mode and a width of 14.7 meV (118 cm^{-1}) for the 130-meV mode.

In this Letter we describe the first high-resolution IR measurement of the ν_1 mode of hydrogen on W(100) at saturation coverage. A surface electromagnetic wave (SEW) spectroscopic technique incorporating a CO_2 tunable laser has been developed to obtain the required surface sensitivity. At room temperature the vibrational mode occurs at 1046 cm^{-1} with a full width at one-half maximum absorption of 14 cm^{-1}, a width which is almost an order of magnitude smaller than that reported in the ELS measurements. The apparent contradiction between the two experiments may be resolved if strong coupling between the ν_1 vibrational mode and surface phonons is involved.

The optical arrangement in our SEW experiment is shown in Fig. 1(a) and described in the caption. The coupling of the SEW to the crystal is shown in more detail in Fig. 1(b). This UHV-compatible geometry combines features from both a recently developed edge-coupling geometry[5] and the traditional two-prism geometry.[6] The coupling depends on the gap, d, between the W(100) and the gold film. After probing 1.3 cm of the W(100) surface, the SEW is decoupled and focused by a short focal length lens (L_2) onto a

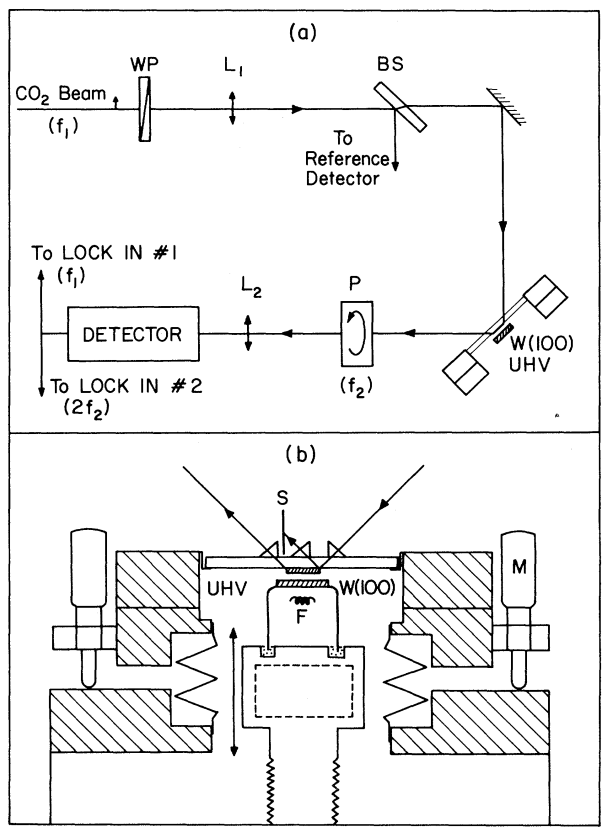

FIG. 1. (a) Schematic drawing of the infrared optics. The CO_2 beam is chopped at f_1 and is polarized. WP is a zero-order wave plate allowing the polarization to be rotated. L_1 and L_2 are lenses. BS is a beam splitter. P is a polarizer rotating at a frequency f_2. (b) Schematic drawing of the window assembly and sample holder. F is a thoriated W filament for electron bombardment of the sample. M is one of the four micrometers, allowing fine positioning of the window with respect to the W(100).

 © 1980 The American Physical Society

pyroelectric detector, as shown in Fig. 1(a). The measurements consist of determining both the change in SEW transmission, ΔI, and the transmission, I. In order to eliminate both the laser intensity and spatial drifts (affecting the coupling), and to enhance the ΔI measurement, we use an optical-bridge technique. When the W crystal is close to the gold film, we rotate the incoming polarization from a purely TM polarized beam to a mixture of TM and TE so that TE waveguide modes are also launched between the gold and tungsten, in addition to the TM-SEW mode. Some of this TE radiation is scattered at the gold-film output edge through the polarizer (P) to the detector. By adjusting the polarization angle, the TE signal, which does not interact with the chemisorbed hydrogen, can be made the same size as the TM-SEW signal which does interact. The output of lock-in No. 2, tuned at $2f_2$, is thus nulled and the sensitivity to small ΔI is increased. Lock-in No. 1, tuned at f_1, records $I_{TM} + I_{TE} = 2I_{TM}$ since the two intensities are balanced.

The W(100) crystal was spark cut and electropolished and then mounted on a Huntington linear-motion feedthrough which had a resolution of 25 μm. The precise adjusting of the window-sample spacing was done with four micrometers as shown in Fig. 2(b). By monitoring the reflection of a He-Ne laser beam both from the sample and from the window, the gold film could be adjusted parallel to the sample to within an infrared wavelength. The gap spacing for optimum signal to noise was found to be 75 μm.

The UHV chamber is pumped by both a 220-liter triode ion pump and a titanium sublimator with a liquid N_2 shield. The working base pressure is typically 1.5×10^{-10} Torr with H_2, He, and CH_4 as principal contaminants. The CO partial pressure was kept below 2×10^{-10} Torr during H_2 exposure.

The sample cleaning procedure consisted of 30-min periods of electron bombardment of the sample at 1200 °C in about 8×10^{-8} Torr O_2, separated by flashes at 2000 °K at 3×10^{-10} Torr. The typical integrated baking time in O_2 was 6 to 10 h. Although our chamber was not equipped with an Auger system we used a crystal cut from the same boule as used by Wojcik *et al.*,[7] who established with Auger spectroscopy that the above described cleaning procedure was more than adequate.

Our Apollo CO_2 laser covers four different frequency regions[8]: 925–955, 970–985, 1037–1054, and 1070–1082 cm^{-1}, with a line approximately at every 2 cm^{-1}. No hydrogen-induced absorption was observed for either of the two lower-frequency branches. In Fig. 2 we show the induced absorption associated with a saturation coverage of hydrogen. The absorption occurs almost entirely in the third laser branch. (Note the discontinuous horizontal axis.) These data can be fitted equally well by a Lorentzian peak at 1046 cm^{-1} with a full width at half maximum (FWHM) of 14 cm^{-1} or by a Gaussian with $2\sigma = 11$ cm^{-1} as shown in Fig. 2.

To obtain the effective charge, e^*, of this ν_1 mode we use the optical sum rule[9] and find $e^* = 0.038 \pm 0.01$ (SEW). This value is in reasonable agreement with the effective charge as calculated from ELS measurements,[10] namely, $e^* \approx 0.04$ (ELS). Both experimental techniques give the same effective charge for the vibrational mode, although the linewidths are very different. This result is to be contrasted with the measurements of CO on Pt(111) where both IR and ELS give the same linewidth.[11] The difference for hydrogen on tungsten is illustrated in Fig. 3. The solid curve labeled IR is a Gaussian fit to our data and the solid points represent the measured spectrum from the ELS measurement.[2]

We now show that the apparent linewidth discrepancy can be resolved by invoking dynamical coupling between the hydrogen and the surface tungsten atoms. Since a saturation coverage of hydrogen does indeed produce a static rearrangement of the surface atoms, such a coupling is reasonable. Linear coupling between the hydrogen vibration and surface phonons would produce

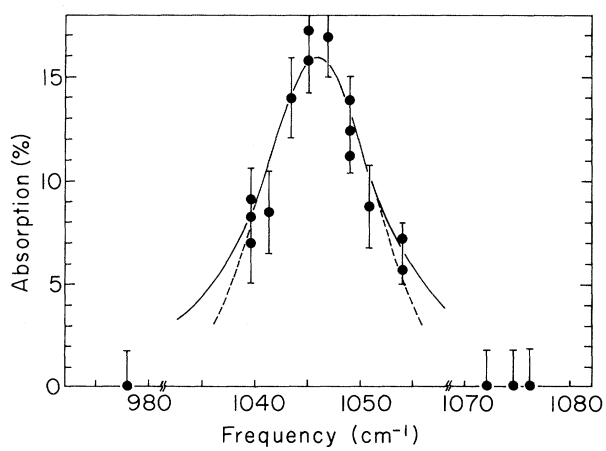

FIG. 2. The hydrogen-induced SEW absorptivity $\Delta I/I$ on W(100) at saturation coverage vs frequency. Note the discontinuous frequency scale. The solid line is the Lorentzian fit and the dashed line the Gaussian fit described in the text.

a characteristic spectrum made up of a sharp zero–surface-phonon transition at ν_1, with an additional broad surface-phonon sideband at higher frequencies corresponding to one–surface-phonon absorption ($\Delta n = +1$) and another band at lower frequencies corresponding to one–surface-phonon emission ($\Delta n = -1$). The absorption coefficient of this band can be written as[12]

$$\alpha(\omega) \sim \omega\delta(\omega - \Omega_1) + \sum_l |(X,l)|^2 \frac{\hbar[n(\omega)+1]}{2}\left(C + \frac{B}{2M^*\Omega_1\omega}\right)^2 \delta(\omega - \Omega_1 - \omega_l)$$
$$+ \sum_l |(X,l)|^2 \frac{\hbar n(\omega)}{2}\left(C - \frac{B}{2M^*\Omega_1\omega}\right)^2 \delta(\omega - \Omega_1 + \omega_l), \quad (1)$$

where the first term represents the zero-phonon ν_1 mode, the second term the $\Delta n = +1$ phonon sideband, and the third term the $\Delta n = -1$ sideband. In Eq. (1), ω is the radiation frequency; Ω_1 is the localized vibrational mode with effective mass M^*; $|(X,l)|^2$ is a coefficient describing the projection of the configurational coordinate onto the surface phonon coordinate q_l with frequencies ω_l; C is the coefficient for second-order dipole coupling; and B is the coefficient for anharmonic coupling.

Unfortunately, the absorption coefficient of the sideband as reflected in the ELS measurement (Fig. 3) is too small to be detected with our current SEW sensitivity, and so we have combined the two sets of data in Fig. 3 to extract the sideband information. Firstly, the resolved (SEW) zero-phonon line is convolved with the ELS instrumental resolution to get the dotted curve C in Fig. 3; next, curve C is subtracted from the ELS spectrum to obtain the sum band spectrum D_+. The spectral information is contained in the solid curve (IR) and the constructed sideband curves (D_+ and D_-). We propose that both ELS and SEW would show the same spectrum if (a) ELS were better resolved and (b) SEW had a better signal-to-noise ratio, and that this spectrum would then look like D_- plus IR plus D_+. It is important to realize that D_+ and D_- will not narrow when the resolution is increased.

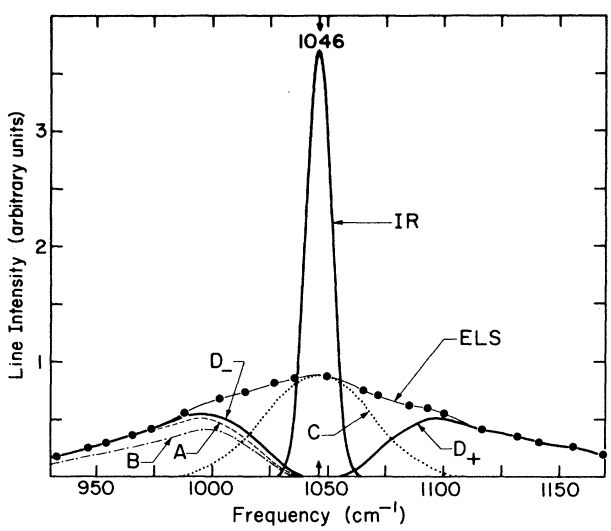

FIG. 3. The ν_1 vibrational band as observed by SEW and ELS. Curve IR is the measured SEW absorption line and curve C the same line convoluted with the ELS resolution function. The lines D_+ and D_- are obtained by subtracting the convoluted IR line (C) from ELS raw data. Line A is the difference sideband obtained from D_+ for the case of a dominant anharmonic coupling, i.e., with Eq. (2), while B is calculated for the case of a dominant second-order dipole moment coupling, i.e., with Eq. (3).

To check for consistency we next examine the difference-band spectrum (D_-). If the anharmonic coupling dominates, $B/2M^*\Omega_1\omega \gg C$, then for each ω_l the ratio of the intensity in the $\Delta n = +1$ sideband to that in the $\Delta n = -1$ sideband is

$$\left.\frac{\alpha(\Delta n = +1)}{\alpha(\Delta n = -1)}\right|_{\omega_l} = \frac{n(\omega_l)+1}{n(\omega_l)}\left(\frac{\Omega_1 - \omega_l}{\Omega_1 + \omega_l}\right)^2, \quad (2)$$

while if the second-order dipole moment dominates then the ratio becomes

$$\left.\frac{\alpha(\Delta n = +1)}{\alpha(\Delta n = -1)}\right|_{\omega_l} = \frac{n(\omega_l)+1}{n(\omega_l)}. \quad (3)$$

The calculated difference-band spectrum as represented by each of these expressions is given in Fig. 3. Satisfactory agreement with the experimental difference band is obtained with the anharmonic coupling.

This dynamical coupling model also provides a natural explanation of the sharper transition observed in ELS at low H coverage. The experimental evidence is that the reconstructed surface of tungsten has a W-H-W bond angle of 89° while the high-coverage β_1 phase has a bond angle of 108°.[3] A simple geometric argument would suggest that the coupling between the surface motion and the perpendicular vibration will decrease as the bond angle decreases. Weak static coupling implies weak dynamic coupling, and most of the intensity would remain in the zero-phonon transition.

With improved sensitivity future high-resolution spectroscopic studies of both the zero-phonon line and its sidebands for a saturation coverage of H on W should provide additional information on the coupling between the two systems.[13] Temperature-dependent studies of the zero-phonon line will probe both the linear and quadratic coupling to the surface phonons; whereas for coupling of the hydrogen to two-dimensional modes, the linewidth should still vary as T^2 at high temperatures, below the Debye temperature it should vary as T^6. Additional information on the density of surface states should be contained in a detailed study of the sideband spectrum.[12]

The authors would like to thank T. W. Capehart, G. W. Graham, Z. Schlesinger, and R. H. Silsbee for many useful discussions and technical advice.

This work was supported by the National Science Foundation through a grant to the Cornell Materials Science Center (Grant No. DMR-76-81083), MSC Report No. 4188.

[a]Present address: Bell Telephone Laboratories, Murray Hill, N. J. 07974.

[1]H. Froitzheim, H. Ibach, and S. Lehwald, Phys. Rev. Lett. 36, 1549 (1976).

[2]A. Adnot and J.-D. Carette, Phys. Rev. Lett. 39, 209 (1977).

[3]M. R. Barnes and R. F. Willis, Phys. Rev. Lett. 41, 1729 (1978).

[4]W. Ho, R. F. Willis, and E. W. Plummer, Phys. Rev. Lett. 40, 1463 (1978).

[5]Y. J. Chabal and A. J. Sievers, Appl. Phys. Lett. 32, 90 (1978).

[6]J. Schoenwald, E. Burstein, and J. M. Elson, Solid State Commun. 12, 185 (1973).

[7]L. A. Wojcik, A. J. Sievers, G. W. Graham, and T. N. Rhodin, to be published.

[8]In order to obtain a nearly Gaussian beam, an aperture was placed inside the laser cavity, thus reducing the range of each laser band.

[9]Y. J. Chabal and A. J. Sievers, J. Vac. Sci. Technol. 15, 638 (1978).

[10]H. Ibach, Surf. Sci. 66, 56 (1977).

[11]R. A. Shigeishi and D. A. King, Surf. Sci. 58, 379 (1976); K. Horn and J. Pritchard, J. Phys. (Paris), Colloq. 38, C4-164 (1977); H.-J. Krebs and H. Luth, Appl. Phys. 14, 337 (1977); H. Froitzheim, H. Hopster, H. Ibach, and S. Lehwald, Appl. Phys. 13, 147 (1977).

[12]M. V. Klein, in *Physics of Color Centers*, edited by W. B. Fowler (Academic, New York, 1968), p. 518.

[13]A. S. Barker, Jr., and A. J. Sievers, Rev. Mod. Phys. 47, S-2 (1975).